Fiber Fabry–Pérot Interferometers Based on Air-Bubbles/Liquid in Hollow Core Fibers

Cheng-Ling Lee, Han-Jung Chang, Yan-Wun You, Guan-Hung Chen, Jui-Ming Hsu, and Jing-Shyang Horng

***Abstract*— This letter develops a miniature and highly sensitive fiber Fabry–Pérot interferometer (FFPI) that is based on an air-bubble and liquid in a hollow core fiber (HCF). The endface of the proposed FFPI is sealed off by an optical fiber plug to ensure the optical/chemical stability of the used liquids. The fiber plug is fabricated with a single-mode fiber taper to close the end of the liquid core fiber. The proposed technique ensures that the filled liquid neither effuses nor becomes contaminated. Experimental results show that the presence of both an air-bubble and liquid in the FFPI enables the highly sensitive measurement of temperature (T), the sensitivity of which can be controlled by changing the ratio of the volume of air to that of liquid in the HCF.**

***Index Terms*— Fiber Fabry–Pérot interferometer (FFPI), hollow core fiber (HCF), liquid core fiber (LCF), fiber taper, fiber-optic component, fiber-optic sensor.**

I. Introduction

AN AIR-BUBBLE or an air-gap that forms in fiber Fabry-Pérot interferometers (FFPIs) acts as micro-cavity that generates low-finesse interference by reflecting from the first and second fiber/air interfaces. Air-bubble-based FFPIs have been investigated and widely utilized in optical fiber parametric sensing [1]–[6], for example, external refractive index (RI) [1], strain [2]–[5] and ambient temperature (T) [1], [5], [6]. Several ellipsoidal or spherical air bubbles have been formed by fusion splicing with single-mode fibers (SMF) or such special fibers as photonic crystal fibers (PCFs). Favorable optical Fabry-Pérot (F-P) interference performance has been achieved using the new structures with the ellipsoidal or spherical air bubbles [1]–[6]. However, the air-bubbles that form in the fibers are always immobile since the air is surrounded by solid silica fiber. The authors recently proposed a novel, dynamic and sensitive liquid core fiber Fabry-Pérot interferometer (LCFFPI) for directional fiber-optic level meters [7] in which the air-bubble drifts. These air-bubbles were moveable in a manner that depended on they floated on the dilute liquid. A configuration in which the air-bubbles are surrounded by liquid in the fiber sensor would be highly temperature-sensitive since thermal expansion coefficients (TEC) of the air and liquid are much higher than that of solid silica. A highly sensitive temperature sensor that is based on an alcohol-filled photonic crystal fiber (PCF) with a PCF length of 6.1cm has been proposed [8]. To investigate the temperature sensitivity of our device in which an air-bubble is surrounded by liquid, a rigid taper plug was used to seal off the LCF end to stabilize the liquid and prevent its contamination by the epoxy, as displayed in Fig. 1. Experimental results show that the presence of both an air-bubble and liquid in the LCFFPI makes the device very sensitive in measuring temperature (T) and that this sensitivity to T strongly depends on the ratio of the volume of air to that of liquid. As T of the surroundings increases, the air bubble that is surrounded by the liquid would be more compressed, enabling more sensitive measurement by monitoring the optical interference dips/peaks shifts.

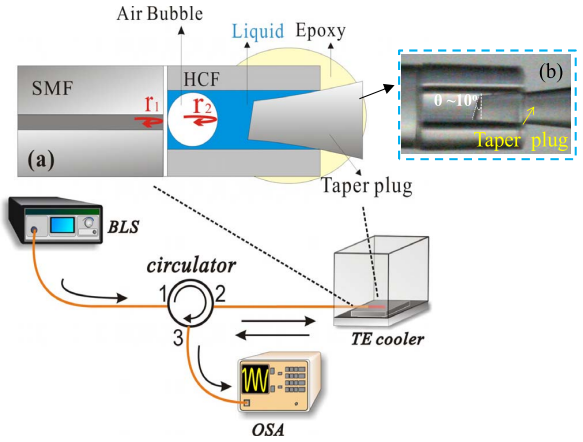

Fig. 1. Experimental setup of the proposed LCFFPI. Inset (a) air-bubble existed inside liquid HCF of sensor tip. Inset (b) microphotograph of proposed non-flat taper plug. BLS: Broadband light source. OSA: Optical spectrum analyzer.

II. Experiment

Fig. 1 presents the experimental setup for making measurements. Inset (a) shows the configuration of the sensor tip and inset (b) displays a microphotograph of the proposed non-flat taper plug for sealing the fiber end. A section of a hollow core fiber (HCF) with core diameter D = 50μm and a length of around 175μm was firstly spliced by a special fusion method. Then, the endface of the HCF was filled by capillary action with Cargille® optical liquid of refractive index (RI) n_D = 1.456. The air in the front section of the HCF gradually formed a spherical air-bubble during the capillary action owing to the surface tension of the filled liquid. The intermolecular cohesive force in the liquid causes the trapped air to form a spherical air-bubble inside the liquid. Fig. 2 shows the evolution of the

Manuscript received November 8, 2013; revised January 7, 2014; accepted January 22, 2014. Date of publication February 4, 2014; date of current version March 20, 2014. This work was supported by the National Science Council of Taiwan under Grant NSC 102-2221-E-239-033-MY3.

The authors are with the Department of Electro-Optical Engineering, National United University, Miaoli 360, Taiwan (e-mail: cherry@nuu.edu.tw; aaron801011@yahoo.com.tw; lovesky791013@gmail.com; jmhsu@nuu.edu.tw; dabow811112@gmail.com; jshorng@nuu.edu.tw).

Color versions of one or more of the figures in this letter are available online at http://ieeexplore.ieee.org.

Digital Object Identifier 10.1109/LPT.2014.2303191

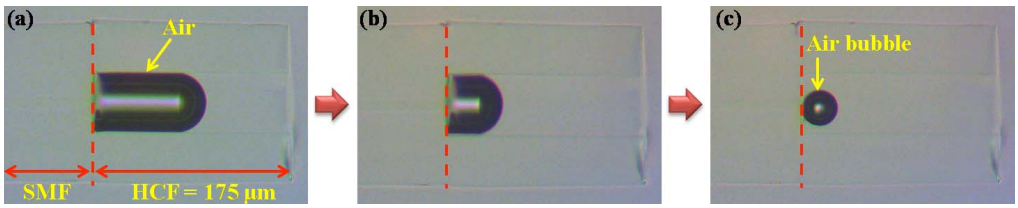

Fig. 2. (a)–(c) Evolution of micro air-bubble that forms in liquid core fiber.

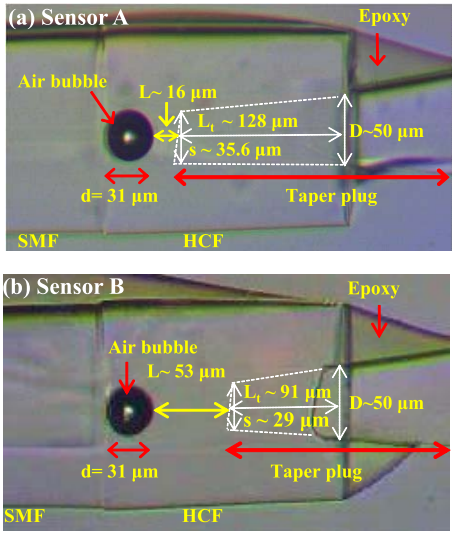

Fig. 3. Micrographs of LCFFPI tips with (a) sensor A: d $\sim$ 31μm, L $\sim$ 16μm and (b) sensor B: d $\sim$ 31μm, L $\sim$ 53μm.

micro air-bubble in the LCF. After the bubble had formed, a size-matched fiber taper plug was inserted into the endface of HCF to close the end. Epoxy was used to seal the end to fix the taper plug and maintain the ratio of the volume of air to that of liquid, as displayed in Fig. 3.

Liquid with a high viscosity coefficient is favored since it is sticky enough to keep the air-bubble attached to the front section of the HCF and it prevents drifting of the air-bubble away from the interface of the SMF and HCF, reducing the interference phenomenon. Permanent stability also can be maintained by packaging the proposed fiber-optic sensor at a slight angle of inclination to ensure that the air-bubble remains close to the SMF. Fig. 3(a) and (b) show two LCFFPIs (sensors A and B, respectively,) which contain air-bubbles of almost equal size but contain different volumes of liquid. The end of the proposed taper plug should be cleaved to form a non-flat surface at a tilt to prevent the undesired Fresnel reflection in the liquid/plug interface. In Fig. 3, d denotes the diameter of the air-bubble; L is the distance between the air-bubble and edge of the plug; s is the diameter of the plug head and L_t is the plug length inside the HCF. Sensor B is plugged by a shorter taper plug; contains more liquid, and so is predicted to have higher T-sensitivity.

III. Experimental Results and Discussion

To study the *T-dependent* variation under expansion of the air/liquid volume ratio in the HCF, the devices herein are

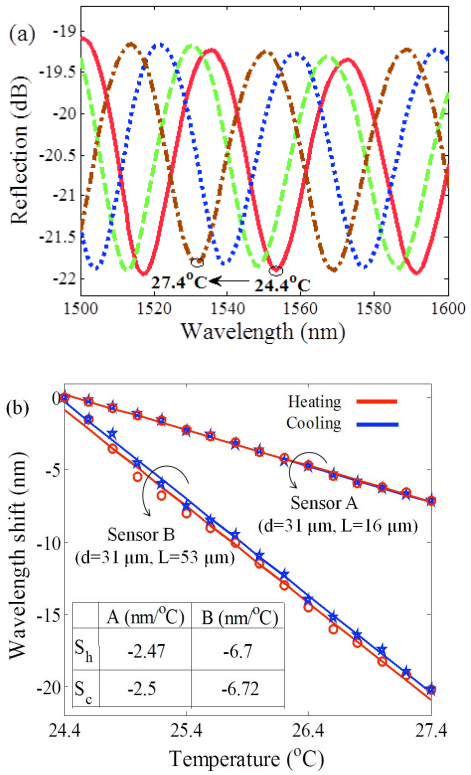

Fig. 4. (a) Variations of reflection spectra of sensor B as T increases (heating). (b) Sensitivity of wavelength shift to temperature during many cycles of measurements for sensors A and B.

packaged at an angle of inclination of 3° and placed on a TE cooler (Resolution: ±0.02 °C) inside a closed space as T is increased from 24.4 °C to 27.4 °C in increments of 0.2 °C. Spectral responses of the sensors are directly obtained using an optical spectrum analyzer (OSA). Owing to the F–P cavity, an air-bubble formed around the liquid, and very sensitive responses to variations in T are estimated to be achievable.

Fig. 4(a) shows the spectral response of sensor B under heating. Sensor B with d $\sim$ 31μm, L $\sim$ 53μm and a shorter taper plug, contains more liquid inside its HCF. Sensors A and B have average experimentally obtained thermal sensitivities $S_{av} \equiv (S_h + S_c)/2$ of about -2.48 nm/°C and -6.71 nm/°C, respectively, as presented in Fig. 4(b), which plots the linear fitted responses of sensors A and B to variations in T, respectively. Here, the parameters S_h and S_c are the average sensitivities for many cycles of heating and cooling, respectively. The measured sensitivities reveal repeatability and good linearity performance for many cycles

TABLE I
SIMULATION RESULTS CONCERNING SENSITIVITY OF PROPOSED LCFFPI DEVICES TO T

Parameters / Devices	L (μm)	d (μm)	L_t (μm)	s (μm)	$V_{air,o}$ (μm^3)	V_{HCF} (μm^3)	V_{liq} (μm^3)	V_{plug} (μm^3)	$V_{air,f}$ (μm^3)	Calculation, S_{cal} (nm/ C)	Experiment, S_{av} (nm/ C)
Sensor A	16	31	128	35.6	15599	343610	133390	194630	15523	2.5214	2.48
Sensor B	53	31	91	29	15599	343610	254830	73187	15401	6.5861	6.71

of measurements over several months, demonstrating the high stability of the devices. According to Fig. 4(b), sensor B, which contains much more liquid than sensor A, has a higher thermal sensitivity. The sensitivity depends strongly on the ratio of the volume of air to that of liquid in the HCF.

Although sensor B has a higher thermal sensitivity, its thermal reversibility and repeatability deviate much more over time because the molecules of air and of the liquid are movable, even at fixed T (in a steady state). Therefore, sensor B, with much more liquid influences and perturbs the air-bubble with more energy, causing greater variation of measurement. The thermal expansion coefficient (TEC) of air is around 1/273 $^{\circ}C^{-1}$ ($+3.663 \times 10^{-3}$ $^{\circ}C^{-1}$) which is a little higher than that of the liquid ($+1.0 \times 10^{3}$ $^{\circ}C^{-1}$). In the sensors, the air and liquid are present together in a closed cavity with a solid, size-matched and fixed fiber taper plug. Therefore, the air-bubble is constricted, and the length of the cavity reduced since the volume of liquid substantially exceeds that of the air-bubble. The thermal variation in the volume is described by the ***Charles' law,*** which describes how gases tend to expand when heated [9].

Since the optical interference is mainly related to the air-bubble cavity, only the change in volume of the air-bubble is considered herein. Thus, the final volume after heating or cooling of the air-bubble is shown below:

$$V_{\text{air,f}} = V_{\text{air,o}} + (V_{\text{air,o}} \cdot \alpha_{\text{air}} - V_{\text{liq}} \cdot \alpha_{\text{liq}}) \cdot \Delta T \qquad (1)$$

Here, $V_{air,o}$ and $V_{air,f}$ represent the original volume of the air-bubble and that after heating/cooling as function of the temperature change ΔT. V_{liq} is the volume of the liquid which is estimated as $V_{liq} = V_{HCF} - V_{air,o} - V_{plug}$, where V_{HCF} and V_{plug} denote the volumes of the hollow core and the taper plug that is inserted in the HCF, respectively. In Eq. (1), α_{air} ($+3.663 \times 10^{-3}$ $^{\circ}C^{-1}$) and α_{liq} ($+1.0 \times 10^{-3}$ $^{\circ}C^{-1}$) are the TEC of air and the liquid, respectively. The terms α_{air} and α_{liq} are positive because the air and liquid tend to expand when heated. However, if the volume of the liquids is several or tens of times that of the airbubble, then the airbubble would be compressed by the expanding liquid in the fixed HCF space. Since the TEC of silica fiber is much lower than that of the air/liquid, thermal effects on the fiber are ignored. As expected, based on the results in Fig. 4(a), the squeezing of the air bubble in a manner determined by the length of the cavity causes a blue-shift in the interference fringes when the device is heated. A reverse shift in the spectra is observed as ambient T is reduced. The wavelength shifts ($\Delta\lambda$) and cavity variation of the air-bubble (Δd) at a specific wavelength (λ) satisfy the relation $\Delta\lambda/\lambda = \Delta d/d$ determines the wavelength

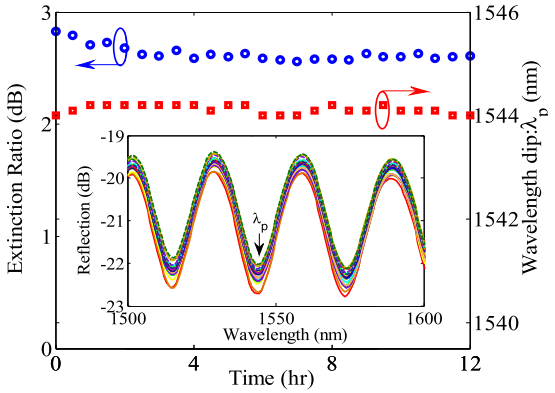

Fig. 5. Extinction ratio (o) and wavelength shift (□) of spectral interference for the device at fixed T of 25 °C over 12 hours. Inset displays spectral variation for long-term sensing with 12hr.

dip shifts (sensitivity) and can be further expressed as,

$$\frac{\Delta\lambda}{\lambda} = \left(\frac{V_{\text{air,f}}}{V_{\text{air,o}}}\right)^{\frac{1}{3}} - 1 \qquad (2)$$

The thermal sensitivity, $S_{cal.} \equiv \frac{\Delta\lambda}{\Delta T}$ (nm/°C), of the device is theoretically determined using Eq. (1) and Eq. (2). Table I presents the calculated values for sensors A and B. Simulation results indicate that the calculated sensitivities $S_{cal.}$ are -2.5214nm/°C and -6.5861nm/°C at λ =1550nm for sensors A and B, respectively. The S_{cal} agrees closely with the experimental results of S_{av}, -2.48nm/°C and -6.71nm/°C, for sensors A and B, respectively.

A packaged sensor was also placed in a room at a fixed T of 25 °C for long-term testing, yielding the results in Fig. 5, which shows interference dips that are generally fixed for 12 hours, with maximal variations of the extinction ratio of the interference fringes and the wavelength dip (λ_p) shift of 0.25dB and 0.2nm, respectively. The inset in Fig. 5 displays the spectral response in detail.

In this letter, differently sized air-bubbles are made by controlling the duration of capillary action and the sealing time of fiber plug. As shown in Fig. 6(a)–(f), when the air-bubble was formed in the LCF, the capillary action was terminated and the taper plug was inserted to close the HCF. Then, the size of the air-bubble remained almost constant because the liquid could not infiltrate into the LCF. However, the plug was little pulled out to reduce slowly the size of the air-bubble since the liquid continued to be slowly squeezed when the HCF end was not completely closed. In the experiments, the device and the fiber plug were fixed on the optical stages and all processes were monitored by a CCD camera, as shown in Fig. 6.

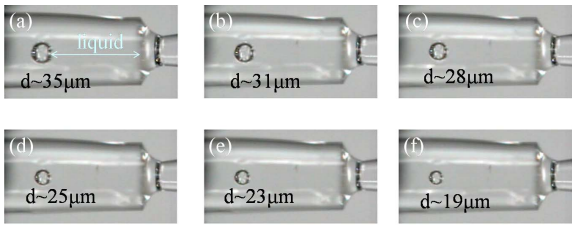

Fig. 6. (a)–(f) Differently sized air-bubbles are obtained when proposed LCFFPI is sealed at various times.

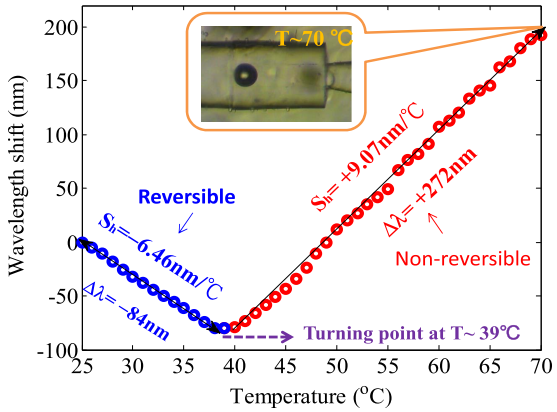

Fig. 7. Wavelength shifts in specific interference dip of sensor B for sensing high T from 25 to 70 °C. Inset presents micrograph of device after heating to T = 70 °C.

This feature increases the flexibility of the proposed fiber device. If the diameter of the air bubble more closely approaches to the used hollow core, then the problem of the air-bubble's having too much space to agitate would be solved. Other diameters of the HCFs can produce air bubbles of differently desired sizes in the devices.

The main shortcoming of the proposed LCFFPI is that its measurement range is limited by the possibility that the filling liquid can break through the fiber taper plug if the internal pressure increases too much upon heating. The measurement range also limited by the free spectral range (FSR) of the interference fringes. Interference dips may overlap under a large T variation. To evaluate the maximal measurement range of the proposed device without considering the overlapped dips, sensor B was well packaged and fixed on a piece of glass with an epoxy-plug to measure high T from 25 to 70 °C (as 70 °C is the highest operating T of the liquid). The spectral shifts are highly linear, exhibiting a blue-shift in the range 25 ∼ 38 °C but a red-shift with increasing T over 39 °C, as plotted in Fig. 7. In the range 25-38 °C, the epoxy-taper plug closes the hollow core, causing the air and liquid therein to remain stationary. Expansion of the liquid squeezes the airbubble in the liquid of the cavity, causing a blue-shift of interference fringes as T increases; this process is thermally reversible. However, the epoxy-taper plug cannot withstand high pressure or high T (>39 °C) since it becomes loose causing the liquid to leak out and air to diffuse in. At the turning point at T ∼ 39 °C, the volumes of the air and liquid cease to be constant. Expansion of the air-bubble squeezes the liquid out through the loosening plug when T is in the range 39-70 °C. Therefore, the red-shift in the interference fringes is deduced to be caused by the expansion of the air-bubble. The inset shows the sensor around T ∼ 70 °C. The expanded air-bubble remains in the hollow core but deformation and irreversibility are evident. We think that problem of the breaking taper plug would be solved by directly tapering the HCF fiber to rigidly seal-off the device [10], and thereby improve the range of measurement of the proposed LCFFPI. In spite of its drawbacks, the proposed device can be developed as an ultra-sensitive T sensor. The proposed taper plug in the HCF is very important as it prevents direct contact between the liquid and the epoxy, and so prevents chemical reactions between them, enhancing the lifetime of the sensor and stabilizing the liquid.

IV. Conclusion

This letter demonstrated an extremely sensitive and in-line LCFFPI based on an air-bubble and liquid together in hollow core fibers. The endfaces of the LCFFPIs are sealed by a fiber taper plug to ensure optical/chemical stability of the liquid therein. The thermal sensitivity of the device can be controlled by changing the ratio of the volume of air to that of liquid. High sensitivity and a linear spectral response with −6.71nm/°C were achieved. The results of theoretical analysis and experimental measurements agree and demonstrate the effectiveness of the sensor. The developed LCFFPI is flexible and ultra-sensitive and it has other favorable characteristics that enable it to be used in sensing other parameters, such as micro-strain, pressure, and angles of tilt.

References

[1] T. Wang and M. Wang, "Fabry–Pérot fiber sensor for simultaneous measurement of refractive index and temperature based on an in-fiber ellipsoidal cavity," *IEEE Photon. Technol. Lett.*, vol. 24, no. 19, pp. 1733–1736, Oct. 1, 2012.

[2] J. Villatoro, V. Finazzi, G. Coviello, and V. Pruneri, "Photonic crystal fiber enabled micro Fabry–Perot interferometer," *Opt. Lett.*, vol. 34, no. 16, pp. 2441–2443, Aug. 2009.

[3] E. Li, G. D. Peng, and X. Ding, "High spatial resolution fiber-optic Fizeau interferometric strain sensor based on an in-fiber spherical microcavity," *Appl. Phys. Lett.*, vol. 92, no. 10, pp. 101117-1–101117-3, Mar. 2008.

[4] F. C. Favero, L. Araujo, G. Bouwmans, V. Finazzi, J. Villatoro, and V. Pruneri, "Spheroidal Fabry–Perot microcavities in optical fibers for high-sensitivity sensing," *Opt. Express*, vol. 20, no. 7, pp. 7112–7118, Mar. 2012.

[5] X. Chen, F. Shen, Z. Wang, Z. Huang, and A. Wang, "Micro-air-gap based intrinsic Fabry–Perot interferometric fiber-optic sensor," *Appl. Opt.*, vol. 45, no. 30, pp. 7760–7766, Oct. 2008.

[6] M. Park, *et al.*, "Ultracompact intrinsic micro air-cavity fiber Mach–Zehnder interferometer," *IEEE Photon. Technol. Lett.*, vol. 21, no. 15, pp. 1027–1029, Aug. 1, 2009.

[7] C. L. Lee, Y. C. Chen, C. L. Ma, H. J. Chang, and C. F. Lee, "Dynamic micro-air-bubble drifted in a liquid core fiber Fabry–Pérot interferometer for directional fiber-optic level meter," *Appl. Phys. Lett.*, vol. 102, no. 19, pp. 193504-1–193504-4, May 2013.

[8] W. Qian, *et al.*, "High-sensitivity temperature sensor based on an alcohol-filled photonic crystal fiber loop mirror," *Opt. Lett.*, vol. 36, no. 9, pp. 1548–1550, May 2011.

[9] P. Fullick, *Physics*, 1st ed. London, U.K.: Heinemann, 1994, pp. 141–142.

[10] L. Ding, C. Belacel, S. Ducci, G. Leo, and I. Favero, "Ultra-low loss single-mode silica tapers manufactured by a microheater," *Appl. Opt.*, vol. 49, pp. 2441–2445, Jan. 2010.